Ensemble of Patches for COVID-19 X-Ray Image Classification

Thiago Dong Chen, Gabriel Bianchin de Oliveira and Zanoni Dias
Institute of Computing, University of Campinas, Campinas, SP, Brazil

Keywords: COVID-19, Deep Learning, X-Ray Images Classification.

Abstract: With the COVID-19 pandemic, several efforts have been made to develop quick and effective diagnoses to assist health professionals in decision-making. In this work, we employed convolutional neural networks to classify chest radiographic images of patients between normal, pneumonia, and COVID-19. We evaluated the division of the images into patches, followed by the ensemble between the specialist networks in each of the image's parts. As a result, our classifier reached 90.67% in the test, surpassing another method in the literature.

1 INTRODUCTION

The new Sars-CoV-2 coronavirus, also known as COVID-19, first discovered in Wuhan (China) in 2019, is a virus capable of producing a dangerous infection and can place high pressure on the health-care system with the need for several hospital beds in hospitals for the recovery of the infected. In March 2020, the World Health Organization (WHO) declared COVID-19 a pandemic, pointing to more than 118,000 cases of coronavirus disease in more than 110 countries and territories around the world and the sustained risk of further spread global (World Health Organization, 2020). Since this statement, there have been drastic changes in the way we live concerning health (Coelho et al., 2020), psycho-social issues (Dubey et al., 2020) and economic (Ozili and Arun, 2020).

With the increase in cases of COVID-19 since its discovery, major impacts on public and private health systems have been taking place, such as the lack of hospital beds and respirators, as well as the lack of RT-PCR tests (Real-Time Reverse-Transcription Polymerase Chain Reaction) (Gibson et al., 1996), which is the most common method to test for potential infected. Even with the RT-PCR method, some cases of false positives and false negatives can happen (Tahamtan and Ardebili, 2020), requiring the evaluation of radiographs and CT scans by specialists, which achieves high rates of effectiveness (Bai et al., 2020; Feng et al., 2020).

X-ray images taken by radiologists have visual characteristics that provide initial indications that the person may be infected with the disease, and these characteristics are usually noticed by specialized physicians. Due to the need to analyze a large number of patient images and the time required for each expert analysis, several efforts have been made to develop efficient and effective methods for the diagnosis of COVID-19.

Driven by their effectiveness in analyzing medical images (Ronneberger et al., 2015; Sato et al., 2020; Teixeira et al., 2020; Zhou et al., 2017), convolutional networks have been seen as a possible alternative to automatically diagnose patients with COVID-19 from chest X-rays (Oliveira et al., 2020).

Some works in the literature deal with the problem of classification of medical images with machine learning and deep learning techniques. Oliveira *et al.* (Oliveira et al., 2020) performed a comparison between different convolutional network architectures, such as ResNet's, EfficientNet's, MobileNet's, and DenseNet's, traditional machine learning classification methods, such as Random Forest, XGBoost, Support Vector Machine (SVM), logistic regression and SVM-Linear, and ensemble techniques, reaching 93.0% in the test set in COVIDx database, version 3. Barstugan *et al.* (Barstugan et al., 2020) developed a COVID computed tomography (CT) image classifier using convolutional networks analyzing patches in different sizes. The extracted characteristics were classified in the SVM model, reaching an accuracy of 98.77% in a database with 150 computed tomography (CT) images. Amyar *et al.* (Amyar et al., 2020) also performed CT image analysis, however, based on multi-task deep machine learning for COVID-19 and pneumonia, performing both segmentation and classification, obtaining an accuracy of 94.67% in the classification task.

With the recent success of patching images (Dosovitskiy et al., 2020), in this work, we evaluate the division of X-ray images into nine patches, with

Chen, T., Oliveira, G. and Dias, Z.
Ensemble of Patches for COVID-19 X-Ray Image Classification.
DOI: 10.5220/0010864500003116
In *Proceedings of the 14th International Conference on Agents and Artificial Intelligence (ICAART 2022) - Volume 3*, pages 561-567
ISBN: 978-989-758-547-0; ISSN: 2184-433X

one specialist convolutional neural network for each patch. After the prediction of each specialist network, we make the ensemble between them. As a result, our method achieved 90.67% of balanced accuracy on the test set, surpassing the classifier developed by Oliveira *et al.* (Oliveira et al., 2020) applied on COVIDx (Wang et al., 2020a), version 7.

The rest of the text is organized as follows. In Section 2, we detail the database applied in this work. In Section 3, we describe the proposed method and the evaluation metric used. In Section 4, we present and discuss the experimental results achieved by our method. In Section 5, we describe the conclusions and possible lines for future work.

2 DATASET

For this work, we used the COVIDx (Wang et al., 2020a) dataset, which is a combination of multiple public database repositories, with images ranging from 157 x 156 resolution to 5623 x 4757. The databases that make up COVIDx are listed below:

- COVID-19 Image Data Collection, COVID-19 Chest X-ray Dataset Initiative (Cohen et al., 2020);
- ActualMed COVID-19 Chest X-ray Dataset Initiative (Wang et al., 2020b);
- RSNA Pneumonia Detection Challenge dataset (Radiological Society of North America, 2019);
- COVID-19 radiography database (Chowdhury et al., 2020; Rahman et al., 2021).

As the COVID-19 X-ray image classification task is a problem of worldwide interest and new radiographs are made every day, the bases that make up COVIDx are constantly updated, adding new images in short periods. Therefore, we chose to use version 7, the latest available in March 2021.

The data set has 15,411 X-ray images, extracted from the thoracic part of the patients, and, for each one of the patients, there may be more than one image. Each X-ray image belongs to one of three possible classes: normal, pneumonia, and COVID. Figure 1 presents example image of each classes.

To divide the data into training, validation, and testing, we applied the same approach indicated in the original repository, i.e., we separated the 300 images designated as test set by the dataset, with 100 images of each one of the classes, and 15,111 remaining for training and validation. These 15,111 remaining images are from different patients from the test set, i.e.

(a) (b) (c)

Figure 1: Example of X-ray image of each class: (a) Normal, (b) Pneumonia, and (c) COVID-19.

there are no images from the same patient into the test set and the 15,111 remaining images.

From the remaining 15,111 images, we divided the patients, ensuring that there were no images of the same patient in training and validation sets. To perform the division, we separated 75% of patients in training and 25% in validation. Regarding the images, the proportion was equal to 74.9% for the training set and 25.1% for the validation set, as shown in Table 1.

Table 1: Number of X-ray images on train, validation and test sets.

Class	Train	Validation	Test
Normal	5,983	1,983	100
Pneumonia	4,123	1,352	100
COVID-19	1,212	458	100
Total	**11,318**	**3,793**	**300**

3 METHODOLOGY

In this section, we describe the steps of the method used for multi-class classification using machine learning techniques. The section is subdivided into preprocessing steps, classification models, and evaluation metric.

3.1 Preprocessing Steps

As the images in the database vary in size, we resized all the data to a dimension of 224 x 224 for the experiments. In addition, we shuffled the data from the training and validation sets to prevent the machine learning model from being biased to some pattern in the ordering of images. Then, we used the preprocessing function indicated for each of the networks pre-trained.

3.1.1 Patches

To evaluate specific regions of the images, we made square cuts with sizes corresponding to 25% of the

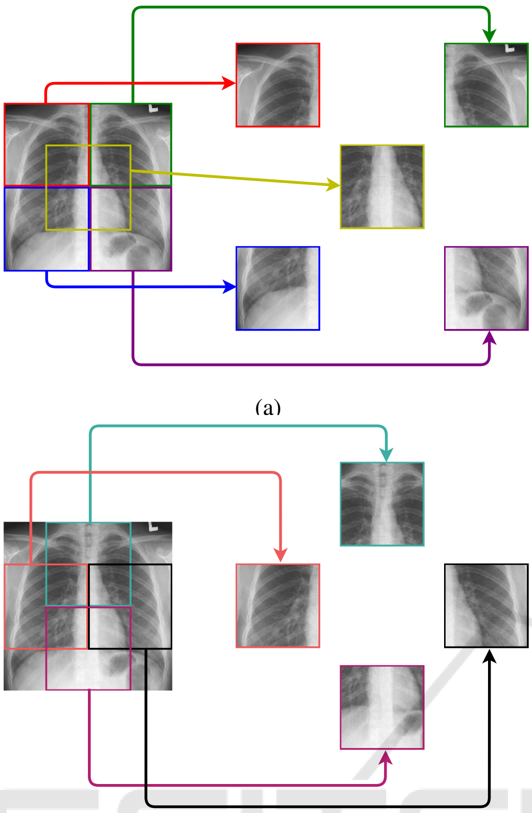

(a) (b)

Figure 2: Representation of patches in the quadrants: (a) top left, top right, bottom left, bottom right, and central. (b) left, right, top, and bottom.

original X-ray (half of the height and half of the width).

We divided each original image into nine regions, or patches, using the four quadrants of the original image, the central region of the image, which has parts of the four quadrants (these five representations are shown in Figure 2a), plus four more regions, created from the intersections between two adjacent quadrants (represented in Figure 2b).

During the experiments, we will refer to the four quadrants as upper left, upper right, lower left, and lower right. For the central region of the image, we will use the term central, while for the intersections between the quadrants, we will employ top, bottom, left, and right terms.

3.1.2 Class Weights

As the training set in the COVIDx database is unbalanced, that is, it does not have the same amount of data for all classes, the most frequent class can bias the training according to the distribution of the data.

To reduce this phenomenon, we applied class weights during training, weighting the error function according to the frequency of samples, making the network “pay more attention” to classes with fewer samples.

To assign weights to each of the classes, we applied Equation 1, where D_{max} represents the amount of data from the most frequent class and D_i represents the amount of data from the i class. By Equation 1, the most frequent class received the weight equal to 1, while the other classes received greater weights.

$$P_i = \frac{D_{max}}{D_i} \tag{1}$$

3.2 Classification Models

In order to make the classification of the X-ray images, we used convolutional neural networks. Figure 3 shows an overview of the methodology applied to classify lung X-ray images, which consists of preprocessing the images and then training the model. After this training step, the model predicts the image into the normal, pneumonia, or COVID-19 class. In this work, we run several experiments to compare the performance of the models with different ensemble techniques. All experiments use stochastic gradient descent as optimizer.

With the success of ResNet50 (He et al., 2016) for lung X-ray image classification (Oliveira et al., 2020), we opted by using this convolutional network for this task. After the preprocessing step, we trained one ResNet50 network for each specific patch of the image. For each convolutional network, we fine-tuned the weights starting from the pre-trained network on ImageNet (Krizhevsky et al., 2012).

After, we evaluated different ensemble techniques for the complete analysis of the lung radiographic images, which consists of the combination of all the specific predictions of different patches of the image.

We performed three types of ensembles from the results of different layers. In the first experiment, we combined the output probabilities of each class of each of the specific models to make the final prediction. In the second experiment, we used the results of the layer before the output layer to carry out the ensemble, which we called deep features, to make the ensemble. In the last experiment, we employed the output prediction of the models to make two voting systems, one using the average of the probabilities of each class by all model, which we called soft voting, and another using the classes predicted by each model, which we call the hard voting.

In the case of the first and the second experiments using ensemble techniques, we applied meta-

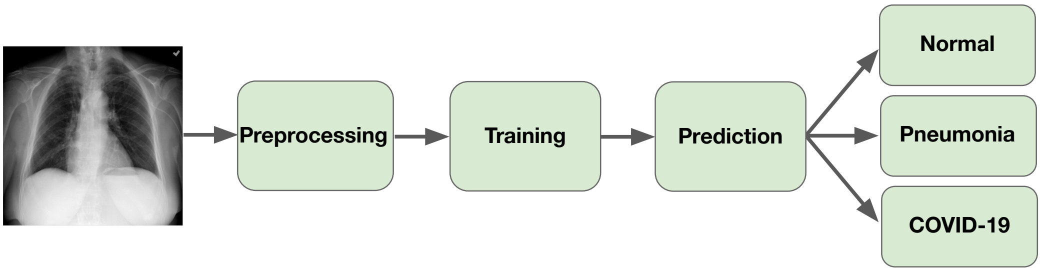

Figure 3: The methodology applied for the classification of lung X-ray images.

classifiers to make the ensemble. Each meta-classifier receives the probabilities or deep features of the nine convolutional networks as input, and it predicts the class between normal, pneumonia, and COVID-19. For the meta-classifiers, we evaluated multi-layer perceptrons with a different number of fully connected layers, varying from one up to three.

3.3 Evaluation Metric

For binary classification problems, recall is the fraction of true positive elements divided by the total number of positively classified units, described in Equation 2, where T_p is the number of true positives and F_p is the number of false positives. True values refer to samples that the model correctly predicted, while false values are those that were incorrectly predicted.

$$Recall = \frac{T_p}{T_p + F_p} \quad (2)$$

In this work, we evaluated the results using the balanced accuracy score, due to that it prevents the result of the predictions of classes with more samples to predominate, in cases where the dataset is unbalanced. The balanced accuracy is essentially the average of the recall values for each class, described in Equation 3.

$$\text{Balanced Acc.} = \frac{1}{3} \times \sum_{i \in \{Normal, Pneumonia, COVID\}} Recall_i \quad (3)$$

4 RESULTS AND DISCUSSION

In this section, we present and discuss the results obtained by our method. We start by choosing the best ensemble technique on the validation set, then we evaluate our method on the test set, apply an explicability technique, and compare our results with the literature.

4.1 Patches

In the first experiment, we evaluated the classification of each patch of the images. Each patch was trained by one specific ResNet50. Table 2 shows the results achieved using each patch, indicating that the region that obtained the best validation accuracy was the central patch, which could happen because of the way the X-ray image is taken, where the lung is centered.

Table 2: Balanced accuracy in the validation set with different patches.

Patch	Balanced Accuracy (%)
Central	91.70
Lower left	91.08
Bottom	91.02
Upper left	90.41
Lower right	90.30
Left	90.00
Top	89.76
Upper right	89.65
Right	88.15

4.2 Ensemble

After the experiments considering each of the patches, we performed the ensemble between them. Table 3 shows the results of each of the ensemble techniques used, indicating higher values of balanced accuracy for all ensemble methods compared to the fine-tuned ResNet50 network on ImageNet and with each of them individually.

Between the ensemble techniques, the best results were achieved by multi-layer perceptron meta-classifier using deep features as input and with three fully connected layers (FCL), which obtained 93.60% of balanced accuracy on the validation set.

4.3 Evaluation on Test

We found our best model found on validation data, which consists of the ResNet50 architecture with

Table 3: Balanced accuracy in the validation set with different ensemble techniques.

Method	Balanced Accuracy (%)
Probabilities	
ResNet50 with 1 FCL	92.87
ResNet50 with 2 FCL	92.39
ResNet50 with 3 FCL	92.19
Deep Features	
ResNet50 with 1 FCL	93.46
ResNet50 with 2 FCL	93.30
ResNet50 with 3 FCL	**93.60**
Voting	
Soft	92.75
Hard	92.76

three fully connected layers using the deep features as input. As a result, we obtained a balanced accuracy score of 90.67% on the test set. This result is slightly lower than the validation accuracy, an acceptable difference meaning that the model manages to generalize adequately.

Then, we analyzed the confusion matrix of the predictions on the test set (Figure 4). The matrix shows that the model obtained good results for all the classes, especially for the normal class. The main errors occurred in the COVID-19 class, where 11% of the images were predicted as pneumonia and 5% of the images were predicted as normal.

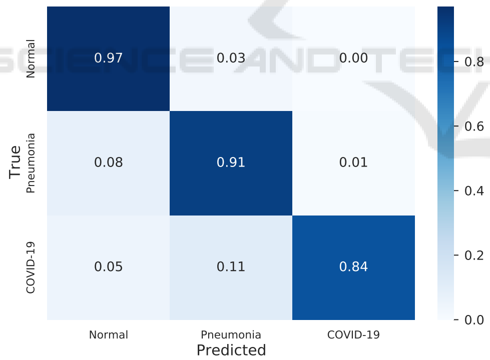

Figure 4: Confusion matrix of our model in the test set.

4.4 Grad-CAM

Grad-CAM (Selvaraju et al., 2017) is a tool that creates a heatmap indicating where CNN is "paying most attention" in the image. To better understand our model, we used Grad-CAM to identify whether the classifier is learning in specific regions in the lungs or if some noise of it X-ray artifact is biasing the model.

Figure 5 shows the Grad-CAM applied to an example input from our test set, using our final model. We can see that the most focused regions are mainly parts of the lung. It is also worth noting that a considerable amount of the images have letters written on the X-ray (this artifact can be seen in the upper right corner of our example, where it has an "L" written on it), however our model managed to ignore the letter.

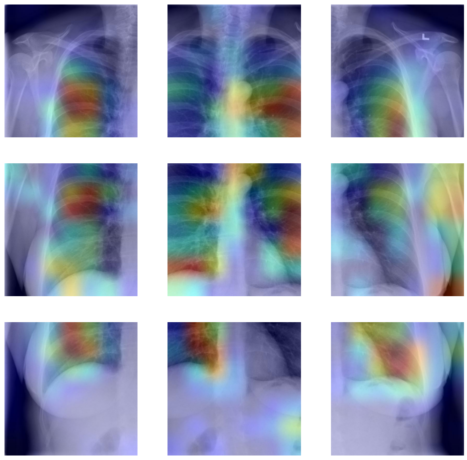

Figure 5: Grad-CAM of the nine patches from an X-ray example on our model. Warmer colors represent greater activation of convolutional network weights.

4.5 Comparison with Literature

To compare our results with the literature, we applied the methodology of Oliveira *et al.* (Oliveira et al., 2020) using the database of this project. We opted for this because there are no works that report results in this version of the COVIDx base, mainly because of its quick update.

With that, this methodology achieved an accuracy of 84.00% in the test set of COVIDx, version 7. Our method reached 6.67 percentage points above this method. Therefore, we conclude that performing the ensemble of the specialist networks in the patches predicts better than using the ensemble with different architectures analyzing the complete image, as the proposed method in Oliveira *et al.* (Oliveira et al., 2020).

5 CONCLUSIONS AND FUTURE WORKS

The pressure on the healthcare system caused by COVID-19 is one of the pandemic's greatest impacts. Those infected need immediate care and treatment. In addition, the prolonged period of the pandemic that people are experiencing exposes the generalized physical, mental and emotional exhaustion suffered by health professionals. Thus, it is necessary to include diagnostic methods that are efficient in helping health professionals.

In this work, we evaluated patching images to improve the results on the classification of lung X-ray images into normal, pneumonia, and COVID-19 classes. Our classification model, which consists of performing an ensemble of the expert models of each patch, presented an accuracy of 90.67% in the test set, allowing us to help in the task of classifying the X-ray images between COVID-19, pneumonia, and normal. The results obtained by our method surpassed the results achieved by another method in the literature applied on COVIDx, version 7.

As future works, the evaluation of more preprocessing steps, as data augmentation, as well as different ensemble techniques, can help the model to achieve better results.

ACKNOWLEDGEMENTS

This research was supported by são Paulo Research Foundation (FAPESP) [grant numbers 2015/11937-9 and 2017/12646-3] and the National Council for Scientific and Technological Development (CNPq) [grant numbers 161015/2021-2 and 304380/2018-0].

REFERENCES

Amyar, A., Modzelewski, R., Li, H., and Ruan, S. (2020). Multi-task deep learning based CT imaging analysis for COVID-19 pneumonia: Classification and segmentation. *Computers in Biology and Medicine*, 126:104037.

Bai, H. X., Hsieh, B., Xiong, Z., Halsey, K., Choi, J. W., Tran, T. M. L., Pan, I., Shi, L.-B., Wang, D.-C., Mei, J., Jiang, X.-L., Zeng, Q.-H., Egglin, T. K., Hu, P.-F., Agarwal, S., Xie, F.-F., Li, S., Healey, T., Atalay, M. K., and Liao, W.-H. (2020). Performance of radiologists in differentiating COVID-19 from non-COVID-19 viral pneumonia at chest CT. *Radiology*, 296(2):E46–E54.

Barstugan, M., Ozkaya, U., and Ozturk, S. (2020). Coronavirus (COVID-19) Classification using CT Images by Machine Learning Methods. *arXiv:2003.09424*, pages 1–10.

Chowdhury, M. E., Rahman, T., Khandakar, A., Mazhar, R., Kadir, M. A., Mahbub, Z. B., Islam, K. R., Khan, M. S., Iqbal, A., Al Emadi, N., Reaz, M. B. I., and Islam, M. T. (2020). Can AI help in screening viral and COVID-19 pneumonia? *IEEE Access*, 8:132665–132676.

Coelho, F. C., Lana, R. M., Cruz, O. G., Codeco, C. T., Villela, D., Bastos, L. S., y Piontti, A. P., Davis, J. T., Vespignani, A., and Gomes, M. F. (2020). Assessing the potential impacts of COVID-19 in Brasil: Mobility, Morbidity and Impact to the Health System. *medRxiv*, pages 1–14.

Cohen, J. P., Morrison, P., and Dao, L. (2020). COVID-19 Image Data Collection. *arXiv:2003.11597*, pages 1–4.

Dosovitskiy, A., Beyer, L., Kolesnikov, A., Weissenborn, D., Zhai, X., Unterthiner, T., Dehghani, M., Minderer, M., Heigold, G., Gelly, S., and Uszkoreit, Jakob abd Houlsby, N. (2020). An image is worth 16x16 words: Transformers for image recognition at scale. *arXiv:2010.11929*, pages 1–22.

Dubey, S., Biswas, P., Ghosh, R., Chatterjee, S., Dubey, M. J., Chatterjee, S., Lahiri, D., and Lavie, C. J. (2020). Psychosocial impact of COVID-19. *Diabetes & Metabolic Syndrome: Clinical Research & Reviews*, 14(5):779–788.

Feng, H., Liu, Y., Lv, M., and Zhong, J. (2020). A case report of COVID-19 with false negative RT-PCR test: necessity of chest CT. *Japanese Journal of Radiology*, 38(5):409–410.

Gibson, U. E., Heid, C. A., and Williams, P. M. (1996). A novel method for real time quantitative RT-PCR. *Genome Research*, 6(10):995–1001.

He, K., Zhang, X., Ren, S., and Sun, J. (2016). Deep residual learning for image recognition. In *Conference on Computer Vision and Pattern Recognition (CVPR)*, pages 770–778. IEEE.

Krizhevsky, A., Sutskever, I., and Hinton, G. E. (2012). ImageNet classification with deep convolutional neural networks. In *Advances in Neural Information Processing Systems (NIPS)*, pages 1097–1105. Curran Associates, Inc.

Oliveira, G., Padilha, R., Dorte, A., Cereda, L., Miyazaki, L., Lopes, M., and Dias, Z. (2020). COVID-19 X-ray Image Diagnostic with Deep Neural Networks. In *2020 Brazilian Symposium on Bioinformatics (BSB)*, pages 57–68. Springer.

Ozili, P. K. and Arun, T. (2020). Spillover of COVID-19: impact on the Global Economy. *SSRN*, pages 1–27.

Radiological Society of North America (2019). RSNA pneumonia detection challenge. https://www.kaggle.com/c/rsna-pneumonia-detection-challenge.

Rahman, T., Khandakar, A., Qiblawey, Y., Tahir, A., Kiranyaz, S., Abul Kashem, S. B., Islam, M. T., Al Maadeed, S., Zughaier, S. M., Khan, M. S., and Chowdhury, M. E. (2021). Exploring the effect of image enhancement techniques on COVID-19 detection using chest X-ray images. *Computers in Biology and Medicine*, 132:104319.

Ronneberger, O., Fischer, P., and Brox, T. (2015). U-Net: Convolutional networks for biomedical image segmentation. In *18th International Conference on Medical Image Computing and Computer-Assisted Intervention (MICCAI)*, pages 234–241. Springer.

Sato, G. T. S., da Silva Segundo, L. B., and Dias, Z. (2020). Classification of musculoskeletal abnormalities with convolutional neural networks. In *2020 Brazilian Symposium on Bioinformatics (BSB)*, pages 69–80. Springer.

Selvaraju, R. R., Cogswell, M., Das, A., Vedantam, R., Parikh, D., and Batra, D. (2017). Grad-CAM: Visual explanations from deep networks via gradient-based localization. In *2017 International Conference on Computer Vision (ICCV)*, pages 618–626.

Tahamtan, A. and Ardebili, A. (2020). Real-time RT-PCR in COVID-19 detection: issues affecting the results. *Expert Review of Molecular Diagnostics*, 20(5):453–454.

Teixeira, V., Braz, L., Pedrini, H., and Dias, Z. (2020). DuaLAnet: Dual Lesion Attention Network for Thoracic Disease Classification in Chest X-Rays. In *27th International Conference on Systems, Signals and Image Processing (IWSSIP)*, pages 69–74. IEEE.

Wang, L., Lin, Z. Q., and Wong, A. (2020a). COVID-Net: a tailored deep convolutional neural network design for detection of COVID-19 cases from chest X-ray images. *Scientific Reports*, 10(1):1–12.

Wang, L., Wong, A., Lin, Z. Q., McInnis, P., Chung, A., and Gunraj, H. (2020b). Actualmed COVID-19 chest X-ray data initiative. https://github.com/agchung/Actualmed-COVID-chestxray-dataset.

World Health Organization (2020). WHO Director-General's opening remarks at the media briefing on COVID-19. https://www.who.int/director-general/speeches/detail/who-director-general-s-opening-remarks-at-the-media-briefing-on-covid-19---11-march-2020.

Zhou, Z., Shin, J., Zhang, L., Gurudu, S., Gotway, M., and Liang, J. (2017). Fine-tuning convolutional neural networks for biomedical image analysis: actively and incrementally. In *Conference on Computer Vision and Pattern Recognition (CVPR)*, pages 7340–7351.